Geomatics for Integrated Coastal Zone Management: multitemporal shoreline analysis and future regional perspective for the Portuguese Central Region

Luca Cenci †, Leonardo Disperati †‡, Lisa P. Sousa ∞, Mike Phillips §, Fátima L. Alves∞

† Centre of GeoTechnologies - CGT, University of Siena, Via Vetri Vecchi 34, 52027, San Giovanni Valdarno (AR), Italy
luqa.cenci@gmail.com

‡ Dipartimento di Scienze Fisiche, della Terra e dell'Ambiente, University of Siena, Via Laterina 8, 53100, Siena, Italy
disperati@unisi.it

∞ CESAM (Centre for Environmental and Marine Studies), Department of Environment and Planning, University of Aveiro, Campus de Santiago, 3830 -193 Aveiro, Portugal
malves@ua.pt; lisa@ua.pt

§ Faculty of Applied Design and Engineering, Swansea Metropolitan University, Mount Pleasant, Swansea, SA1 6ED, Wales, UK
m.phillips@smu.ac.uk

www.cerf-jcr.org

www.JCRonline.org

ABSTRACT

Cenci, L., Disperati, L., Sousa, L.P., Phillips, M. and Alves, F.L., 2013. Geomatics for Integrated Coastal Zone Management: multitemporal shoreline analysis and future regional perspective for the Portuguese Central Region. *Proceedings 12th International Coastal Symposium* (Plymouth, England), *Journal of Coastal Research*, Special Issue No. 65, pp. 1349-1354, ISSN 0749-0208.

Shoreline mapping and change detection are critical for Integrated Coastal Zone Management (ICZM) and all that it represents. This research utilized previous studies that combined both Remote Sensing and Geographical Information System (GIS) techniques to assess, map and forecast shoreline evolution from short-term perspectives. The study area is located in the central region of Portugal, between the counties of Ovar and Marinha Grande (*circa* 140 km) and the time period assessed was from 1984 to 2011. Historical data were used to calculate advance and retreat rates in order to support environmental scenarios for the Portuguese Central Region's Coastal Management Plan. To ensure accuracy, a repeatable procedure was validated using Landsat TM and ETM+ satellite images, which were subsequently enhanced and elaborated by Remote Sensing analyses to detect and extract shorelines. They were subsequently integrated within an Esri ArcGIS software application (DSAS - Digital Shoreline Analysis System) to determine and predict rates of coastline change. Graphical DSAS plots identified coastline phases and shifts and were used to simulate the 2022 coastline scenario. These results will be integrated into the Coastal Zone Management Plan (Horizon – 2022). Importantly this methodological planning approach provides visual coastline change information for regional decision-makers and stakeholders.

ADDITIONAL INDEX WORDS: *Remote sensing (RS), GIS, Landsat, coastal erosion, erosion rate, shoreline evolution, shoreline prediction, coastal management.*

INTRODUCTION

Worldwide coastal zones are experiencing significant transformations due to climate change (*e.g.* sea level rise, increase of tropical cyclone intensity) and anthropogenic interventions (*e.g.* urbanization, reduced sediment delivery to the coast) (Roebeling *et al*., 2011). Despite more than 40% of world population living in coastal areas, it represents only 20% of all land in the world (Martinez *et al*., 2007), meaning that the economic value of these areas and risks associated with coastal erosion are high. In this framework concepts such as "vulnerability" and "risk zones" need to be precisely defined and estimated in order to support political and technical decisions (Alves *et al*., 2007). The evolution of shoreline position through time is a matter of great importance for coastal zone management purposes because coastal managers require information about where the shoreline is located, where it has been in the past, and where it is predicted to be in the future (Boak and Turner, 2005). The objective of this paper is to adopt a procedure based on integration of geomatics data and tools to perform multitemporal shoreline analysis of the central region of Portugal (Ovar-Marinha Grande) in order to obtain predictive short-term future scenarios to quantitatively support the region's Coastal Zone Management Plan.

STUDY AREA

The study area (Figure 1) is located in the central coastal region of Portugal, between the counties of Ovar and Marinha Grande (ca. 140 km). It is a wide coastal plain, oriented approximately N21°E, made up of medium to coarse sand and dune system resting on top of both Pliocene-Quaternary sediments and Mesozoic rocks (MAMAOT/APA I.P., 2012). Shoreline continuity is interrupted by the Ria de Aveiro lagoon with its artificial harbour, the cliff of Serra da Boa Viagem (258 m asl) located to the North of the Figueira da Foz harbour and the cliff of São Pedro de Moel. Only a small percentage (< 4%) of the study area is represented by these cliffs where Mesozoic rocks crop out.

DOI: 10.2112/SI65-228.1 received 07 December 2012; accepted 06 March 2013.

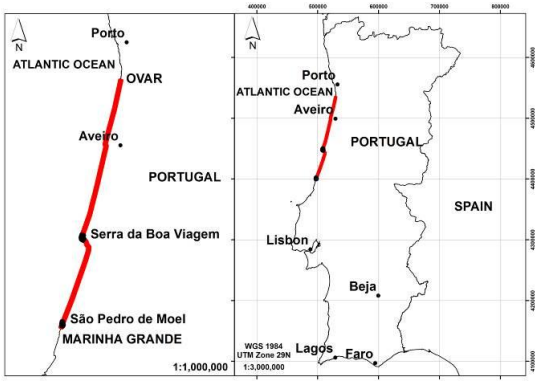

Figure 1. Study area (thick line).

According to Silva *et al*. (2009), in the northern sector of the study area (Mira - Aveiro), the beach area slope ranges between 0.07 and 0.09.

Regarding vegetation cover a typical transverse profile moving toward inland, is characterised by three features: the beach, seaward dune area covered by scattered vegetation and inward stable dune area covered by dense vegetation. Scattered vegetation may be very narrow-absent or it may reach up to *circa* 300 m width. In these latter cases areas correspond to the psammophila vegetation habitats as described in MAMAOT/APA I.P. (2012). The wave regime is mainly north-west oriented with 2 m mean wave height and 12 s mean wave period; storm waves may reach 8 m height and may persist for up to 5 days. The tide regime is semi-diurnal with a spring tidal range between 2 and 4 m and longshore transport, mainly due to wave action, is southwards (Veloso-Gomes *et al*., 2006; Silva *et al*., 2009). Central Portuguese coastal erosion is severe and mainly due to: urbanization of natural areas, coastal defence interventions, port construction works (e.g. Aveiro harbour) and reduced sediment supply (Coelho *et al*., 2009). The latter results from diminished sediment loads from the Douro river that under natural conditions supplies between 1.5 and 2.0 x 10^6 m^3 y^{-1}, but in recent times has reduced supply to < 0.25 x 10^6 m^3 y^{-1} (Bettencourt, 1997). This change was caused by in-river works and actions (*e.g*. dam construction, navigation dredging, sand extraction and river shore protection), as well as catchment land use and practice changes (Coelho *et al*., 2009; Roebeling *et al*., 2011).

METHODS

The coastline is extremely dynamic because many processes affect both its position and shape, e.g. sea level, tides, atmospheric pressure, storms, off-shore and on-shore morphology, longshore drift and vegetation cycles. Hence, when quantitatively assessing shoreline evolution, features coherent in space and time should be analysed in order to reduce misinterpretation. For these reasons in the literature several "shoreline" definition-proxies are considered such as high water line, wet-dry line, base/top of bluff/cliff, vegetation line, etc. (Boak and Turner, 2005; Milli and Surace, 2011). In most cases the choice of proxy depends on several factors such as coastal location, data source and researcher preference (Morton *et al*., 2004). Another issue is the technique used to analyse shoreline evolution, as although most techniques are similar, methodological variations exist which may lead to significantly different results, even when working on the same coastline (Crowell *et al*., 1993). In this work, based on characteristics of the coastal area under study and available archive data, the stable dune vegetation line was considered as the shoreline proxy since it may be regarded as a good erosion indicator (Boak and Turner, 2005). A radiometric analysis of a multitemporal dataset of Landsat imagery allowed the identification and location of this proxy. Finally, by means of geomatic procedures, shoreline evolution in the study area was evaluated over time and a 2022 scenario simulated.

Data Source

The USGS freely offers for downloading from 1972 onwards, the archive of orthorectified MSS, TM and ETM+ imagery acquired by Landsat 1-5 and 7 (NASAa, 2012). After a selection based on image availability, radiometric quality and cloud cover, Landsat images described in Table 1 were downloaded. Taking into account shoreline retreat rates obtained from aerial photograph interpretation between 1947 and 1990 in the Aveiro-Cape Mondego stretch (up to 4.5 m/y; Ferreira and Dias,1992) Landsat data, having spatial resolution of 30 m, were considered adequate for performing a multi-temporal shoreline analysis. In order to obtain a reliable change detection estimate, the multitemporal image dataset was geometrically co-registered and radiometrically normalised (Lunetta and Elvidge, 1998 amongst others). Moreover, 2011 natural colour digital orthophotos with a spatial resolution of 0.5 m (National Environment Agency, formerly INAG I.P) and covering the whole study area, were used.

Geometric Co-Registration

Images downloaded from Landsat free archive were processed through the Level-1 Product Generation System (LPGS), classified as Level 1T product (Standard Terrain Correction) and georeferenced to the Universal Transverse Mercator (UTM) map projection system, zone 29 North (WGS84 Datum). Images were provided with metadata which include residuals of GCPs used to perform orthorectification, the Root Mean Square Error (RMSe) for every image quadrant and for the overall scene (NASAb, 2012). To assess the geometric co-registration quality of the images, residuals were analysed related to the study area GCPs (results in Table 1). Considering Landsat TM pixel size, these values were considered acceptable (smaller than half the pixel size) and no further image spatial co-registration was considered necessary.

Radiometric Co-Registration

The image data were firstly converted from calibrated Digital Numbers (DNs) to at-sensor spectral radiance by using the equations and rescaling factors of Chander *et al.* (2009). However, output images are still affected by atmosphere and illumination geometry effects (Schowengerdt, 2007) which results in errors when making comparisons between images acquired in different epochs. For this reason there are many authors who approached the issue of radiometric absolute or relative correction (e.g. Chavez, 1988; Schott *et al*., 1988; Yang and Lo, 2000; Song *et al*., 2001; Hadjimitsis *et al*., 2004; Mahiny and Turner, 2007;

Table 1. Dataset of Landsat imagery and Root Mean Square Error (RMSe) in the study area subset.

Sensor	Acquisition epoch	RMSe (m)
TM 5	09/08/1984	7.95
TM 5	07/31/1987	7.33
ETM +	06/24/2000	1.06
TM 5	08/12/2003	5.04
TM 5	08/07/2007	6.84
TM 5	10/15/2009	6.78
TM 5	10/05/2011	7.63

Hadjimitsis *et al*.,2010). Despite the specific analytical procedure implemented, in order to perform absolute corrections, atmosphere transmissivity properties need to be known. Because the atmospheric parameters to make a reasonable absolute conversion from at-sensor spectral radiance to surface reflectance were unknown, it was decided to mitigate atmospheric effects and subsequently perform a Relative Radiometric Normalization (RRN). The first step involved applying the Dark Object Subtraction (DOS) approach (Song *et al*., 2001). Deep clear water bodies and shadow areas located near the coast were selected as Dark Objects to take into account effects due to oceanic atmospheric conditions. The second step (RRN) consists of a pixel-based multiband normalization of every image in respect to a reference image selected within the dataset. In doing so the residual radiometric differences between the images, mainly related to changes of illumination conditions due to different Day-Of-Year (DOY; Table 1), are mitigated because they are equalised to the reference image (Yuan and Elvidge, 1996; Yang and Lo, 2000). For this study, RRN consisted of linear regression normalization based on Pseudo Invariant Features (PIFs), e.g. man-made objects such as street or roofs whose reflectance should be constant through time (Schott *et al*., 1988), and hence changes through time of at-sensor-radiance are assumed to be artefacts. In the RRN one image is considered as "reference" while others are considered "slave" because their radiometry will be adjusted to match the reference (Lunetta and Elvidge, 1998). By plotting PIFs values of reference and slave images slope and intercept coefficients were obtained to adjust the slave radiometry to the reference (Lunetta and Elvidge, 1998; Schott *et al*., 1988; Yuan and Elvidge, 1996; Yang and Lo, 2000). In this work PIFs were selected by visual interpretation following these criteria (Eckhardt *et al*., 1990). They are located at approximately the same elevation in relatively flat areas so that atmospheric thickness over each target is approximately the same and the sun angle between images does not produce different effects. Furthermore PIFs were selected in order to have a wide range of radiance values to obtain a reliable regression model. The 2003 image was chosen as reference because for a large image dataset that covers a long time period, it is preferable to select a reference image closest to the middle of the time sequence to minimize land cover/use differences (Yang and Lo, 2000). This procedure allowed the obtaining of a dataset geometrically co-registered and radiometrically normalised to the 2003 epoch image.

Shoreline Definition And Mapping

One of the main aims of this research was to develop and apply a robust and repeatable procedure to detect and delineate the chosen ''shoreline'' feature within the available data source (Boak and Turner, 2005). In this study shoreline proxy related to the beach-ocean boundary (e.g. high water line or wet-dry line) which is subjected to strong daily tidal influences that may lead to changes up to 40-50 m in the position of low/high tide marks (Ferreira and Dias, 1992). Consequently, it was decided to adopt as a shoreline proxy the vegetation line defined as separating dune areas and mainly covered by dense and stable vegetation, unlike seaward areas mainly covered by scattered vegetation (as e.g. Thomas *et al*., 2011). Furthermore by using this proxy, the effects on Landsat imagery radiance of the phenology cycle were mitigated, which was assumed to be of more importance in dune areas covered by scattered vegetation. Cliffs were excluded from shoreline change analyses because corresponding retreat rates were considered undetectable over the given time span when using low spatial resolution Landsat imagery. Urban coastal settlements were also excluded because these areas have always been protected by engineering infrastructure so they are not representative of shoreline evolution. Additionally, excluded areas represent *circa* 26 km, less than the 20% of the study area. To identify the proxy, the vegetation line was first mapped onto the 2011 orthophotos by visual interpretation of different physiographic sample areas representative of the different kinds of transition between beach and stable vegetation. The delineation process was independently repeated to obtain a set of lines aimed at evaluating the positional uncertainty associated with visual interpretation. The Difference Vegetation Index (DVI = NIR-R; Lillesand and Kiefer, 1987) was calculated from the 2011 Landsat image. Subsequently, the DVI threshold value to obtain the best fit was chosen with the median vegetation line position previously delineated from the orthophotos. In order to define this value, reference data was sampled by using a bilinear interpolation: 1300 pixels clusters equally located seaward and landward to that line. Finally the threshold value as median of the statistical population was chosen (Figure 2). By comparing the line visually delineated on the orthophotos to the line obtained by thresholding the DVI image, a mean distance of 12 m was found. This value being smaller than 0.5 pixel, the DVI-based Vegetation Line (DVI-VL) was considered representative of the chosen proxy. By applying the same DVI threshold to the whole image dataset a first multi-temporal raster representation of the DVI-VL was obtained. The final vector representation of the DVI-VL was obtained by applying GIS raster to vector conversion and line generalisation procedures. Following previous steps seven DVI-VLs were obtained and subsequently used to determine rates of shoreline change.

Uncertainty

Trends and rates of shoreline change are only as reliable as measurement errors that determine the accuracy of each shoreline position (Hapke *et al*., 2006), and there are several uncertainty sources that may influence historical shoreline mapping and change rates (Fletcher *et al*, 2003). In this study, the Pixel Error (***P***), Geometric Error (***G***), Digitizing Error (***D***), and DVI-Threshold Error (***DVIT***) were considered as sources of uncertainty:

- **Pixel Error** (***P***): Assumed to be equal to the pixel size (30 m) because in theory, it is not possible to resolve features smaller than this value (Virdis *et al*., 2012).
- **Geometric Error** (***G***): Calculated from the residual of the

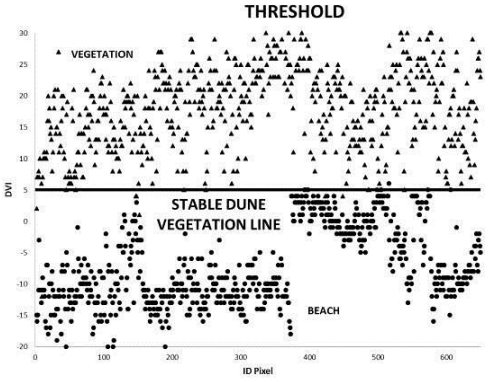

Figure 2. Dataset of reference clusters sampled to obtain the DVI threshold value (5) from DVI image of 2011. Circles represent clusters classified as beach with scattered vegetation while triangles represent clusters dominated by stable vegetation.

study area GCPs provided with image metadata (Table 1).

- **Digitizing Error** (***D***): Evaluated by delineating the same feature, on the same image, several times and calculating the error as the standard deviation of position residuals for that feature (Virdis *et al*., 2012). This source of uncertainty is assessed by comparing positions of the different vegetation lines obtained by visual interpretation of the 2011 orthophotos (5 m).
- **DVI-threshold error** (***DVIT***): This source of uncertainty is evaluated by taking into account the average residual between the reference vegetation line and the DVI-VL (12 m).

These errors were assumed to be uncorrelated and random, and quantified by calculating the square root of the sum of the squares of all uncertainty factors (Fletcher *et al*., 2003):

$$U = \sqrt{P^2 + G^2 + D^2 + DVIT^2} \quad (1)$$

Sources of uncertainty, except for ***G***, are independent from the image acquisition epoch. Hence for ***U*** a constant value of 34 m, calculated from the maximum value of ***G***, was assumed.

Estimation Of Shoreline Change Rates

To calculate shoreline change rate, the Digital Shoreline Analysis System (DSAS), a freely available software application that computes rate-of-change statistics for a time series of shoreline vector data, was used (Thieler *et al*., 2009). Four types of change-statistics were calculated by referencing shorelines to an arbitrary onshore baseline located by casting 100 m spaced transects: Net Shoreline Movement (NSM), End Point Rate (EPR), Linear Regression Rate (LRR) and Weighted Linear Regression rate (WLR). The first represents net movement of the vegetation line over time, while the others represent the rate of change in m/y (for a wider explanation of these statistics, see Thieler *et al*., 2009). Since uncertainty was considered to be constant for every dataset image, it was decided to adopt the results of LRR to estimate the shoreline evolution trend. LRR/Transects were then plotted and the function interpolating data was found in order to reduce local noise (Figure 3). New smoothed LRR values were then associated to further transects to represent final LRR values along the shoreline (Figure 3). DSAS also provides the R-squared value that describes how much the rate of each transect is "reliable" according to linear regression (Thieler *et al*., 2009; Figure 3).

Future Shoreline Scenario

Future shoreline scenarios are one of the inputs within the framework of European Recommendations on Integrated Coastal Zone Management and many authors deal with future shoreline scenarios (e.g. Fenster *et al*., 1993; Crowell at al., 1997; Li *et al*., 2001; Ferreira et. al., 2006; Goncalves, 2012; Mukhopadhyay, 2012). After Fenster *et al*. (1993) the observed periodical rate of shoreline change is a reasonable parameter for the estimation of the future shoreline position. In fact this empirical approach does not need to implement other parameters such as sediment transport or wave interference because the cumulative effect of all the processes involved in the coastal dynamics are assumed to be represented by the position history (Li *et al*., 2001). In this work, final LRR trends (e.g. Figure 3) were used to extrapolate an informed 2022 DVI-VL scenario.

RESULTS AND DISCUSSION

Landsat images have been widely used by coastal researchers to study shoreline movements and rates (e.g. White and El Asmar, 1998; Mukhopadhyay, 2012). Limitations dictated by their coarse spatial resolution (30 m) are mitigated by their synoptic, multitemporal and multispectral information. In this study results show that 30 m pixel size is adequate for measurement and spatial analysis of the shoreline change signal over about 30 years time span. The reliability of results obtained from the LRR is evaluated by R-squared (LR2) in Table 2, spatially visualised in figure 3: more than 65% of transects used for shoreline evolution analysis are characterised by LR2 > 0.7. This result and interpolation functions of the time series associated with shoreline positions suggest that shoreline changes follow a near linear trend, indicating the robustness of the method. Obviously it cannot be excluded that wider time span and higher temporal resolution

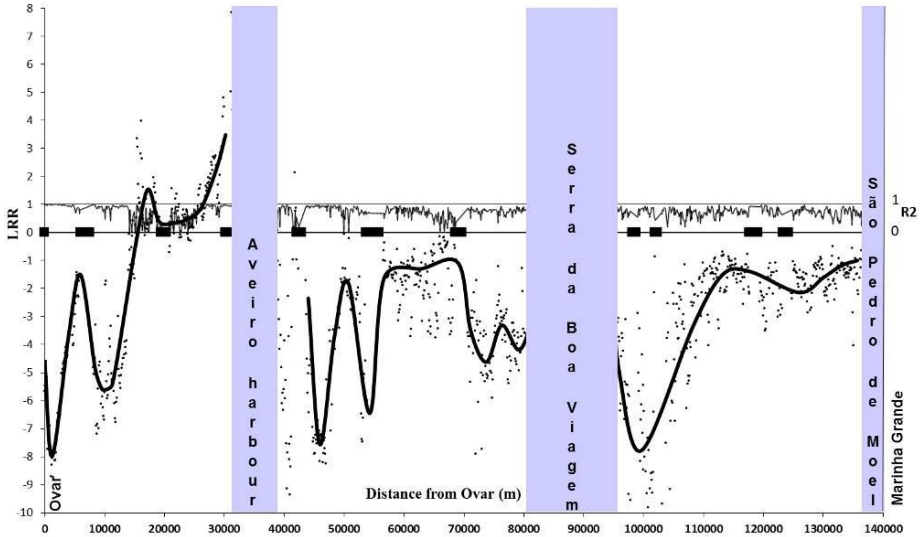

Figure 3. LRR estimation (points) and interpolation (thicker line). Gray stripes represent areas excluded from shoreline change analyses (cliffs and the Aveiro harbour). Thinner line represents R-squared values. Black rectangles represent urban settlements. Statistics in urban areas were not calculated hence lines in urban areas were obtained by interpolation only for visual representation of the functions.

Table 2. LRR and LR2 statistics. Negative values of LRR denote retreat, positive values of LRR denote advance.

LRR	% of transects	LR2	% of transects
< -7	8%	**< 0.5**	13%
-7 - -3	32%	**0.5 - 0.7**	21%
-3 - 0	45%	**> 0.7**	66%
0 - 3	12%		
3 - 7	2%		
> 7	1%		

could enhance recognising non-linear trends. Further studies may be undertaken in order to better understand this issue.

By observing the LRR (Table 2) it can also be seen that the DVI-VL is generally retreating (Figure 4). The DVI-VL shows advancement almost exclusively along the coastal stretch located to the North of the harbour of Aveiro. A comparison with previous work by Ferreira and Dias (1992) for the Aveiro-Cape Mondego Area, estimated shoreline change rates from 1947 to 1990 by using as proxy, the beach-dune interface mapped through aerial photographs and making predictions to 2020. Rates predicted for the stretch Vagueira - Areão for 1990-2010 are -5.4 m/y, agreeing with study results for the same area (average value: -6 m/y, Figure 4). From Areão to Tocha predicted rates for the same period are progressively smaller (-2.2÷-0.4 m/y), again reasonably agreeing with these results (average value: -2 m/y). However, for the smaller area to the south of Tocha, nearly stable predicted shoreline conditions (-0.2 m/y) differed from study results which showed a significant retreat trend (average value: -3.7 m/y). It is concluded that in general, agreement is observed when working with different shoreline proxies extracted from various data sources and processing methods. Furthermore, differences around Tocha may also suggest that results may mismatch if different proxies do not follow similar evolution along the same coastline stretch. Regarding the meaning and interpretation of the general retreat identified by the DVI-VL shoreline proxy (Table 2), it is argued that coastal vegetation cover has progressively reduced its role as beach protection. This condition may be associated to the occurrence of active erosion processes which should be carefully checked by means of other independent evaluation/measurement tools. Further studies based on the analysis of other shoreline proxies are suggested to support study results. The predicted 2022 scenario is reasonable for the typical cross-shore profile comprising beach, scattered vegetation and stable denser vegetation, and if no significant coastal engineering constructions or interventions are built. Deviations from these predictions may be otherwise expected. However, in order to accurately assess predictions, the evolution of the littoral should be monitored, and other methods of predicting future scenarios should be used for a comparison and robustness check (e.g. Gonçalves *et al*., 2012). Uncertainties caused by human intervention may be inferred by temporal shoreline change and 2022 predictions (Figure 4). Although the beach width increases adjacent to transverse engineering works, both beach width increase and shoreline retreat occur. This condition highlights that special attention should be paid when assessing coastline stretches where the balance between along- and cross-shore processes can be affected by anthropogenic actions. Distinguish between natural rates and those influenced by human actions is crucial when historical rates of change are used for Coastal Zone Management purposes. To this aim, monitoring shoreline positions before and after human interventions could be a first step to better understand this issue (Hapke *et al*., 2006).

Figure 4 LRR statistics and example of 2022 scenario. Negative values of LRR denote retreat, positive values of LRR denote advance.

CONCLUSION

The main goal of this research was to develop and validate a geomatic approach for shoreline change analyses to predict evolutionary scenarios. The methodology used should lead to a robust and repeatable procedure to detect a chosen ‘‘shoreline’’ feature according to available data (Boak and Turner, 2005) and study area characteristics. This objective was achieved by implementation of a semi-automatic procedure based on the identification of a DVI threshold value allowing the obtaining of a representation of the vegetation line proxy. Compared to traditional procedures of visual shoreline delineation, the semi-automatic procedure is time saving for regional scale analyses and is less user-dependent: hence more objective and repeatable. Another advantage of this modus-operandi, within areas where the change signal is in the order of tens of meters, is that the data cost is nil, because Landsat images covering a long time span, may be used free of charge. Furthermore the method allows inclusion of images with different spatial or temporal resolution within the same source dataset. By applying this method, shoreline change rates have been evaluated in the Central Region of Portugal (Ovar - Marinha Grande) and a general trend of retreat was identified (average LRR rates ca. -3 m/y; maximum ca. 10 m/y). Furthermore, a future short term scenario was simulated according to these LRR rates.

ACKNOWLEDGEMENTS

We thank the EU Lifelong Learning Programme for supporting the traineeship of L. Cenci at the Department of Environment and Planning, University of Aveiro, within the Erasmus Placement framework, under the supervision of L. Disperati and F.L. Alves.

We thank also the Technical Team of the POOC Ovar-Marinha Grande - CEDRU/UA.

LITERATURE CITED

Alves, M.F.L., Pereira da Silva, C. and Pinto, P., 2007. The Assessment of Coastal Zone Development at a Regional Level – the case study of the Portuguese Central Area. Journal of Coastal Research, Special Issue, 50, 72-76.

Bettencourt, P., 1997. Notas para uma estratégia de gestão da orla costeira. In: Carvalho G.S. (ed.): Colectânea de Ideias Sobre a Zona Costeira de Portugal. Associação Eurocoast-Portugal (AEP), Porto, Portugal. 265-283.

Boak, E.H. and Turner, I.L., 2005. Shoreline definition and detection: a review. Journal of Coastal Research, 21(4), 688–703.

Chander, G., Markham, B.L. and Helder, D.L., 2009. Summary of current radiometric calibration coefficients for Landsat MSS, TM, ETM+, and EO-1 ALI sensors. Remote Sensing of Environment,113, 893-903.

Chavez, P.S.Jr., 1988. An improved dark-object subtraction technique for atmospheric scattering correction of multi spectral data. Remote Sensing of Environment, 24, 459–479.

Coelho, C. and Veloso-Gomes, F., 2006. Crosshore beach profile models - application to Aveiro coast. Journal of Coastal Research, 39, 345 - 350.

Coelho, C., Conceição, T. and Ribeiro, B., 2009. Coastal erosion due to anthropogenic impacts on sediment transport in Douro River – Portugal. Proceedings of the Coastal Dynamics 2009 conference, Tokyo, Japan. Paper 72, 15p.

Crowell, M., Douglas B.C. and Leatherman, S.P., 1997. On Forecasting Future U.S. Shoreline Positions: A Test of Algorithms. Journal of Coastal Research, 13(4), 1245-1255.

Crowell, M., Leatherman, S.P. and Buckley, M.K., 1993. Shoreline Change Rate Analysis: Long Term Versus Short Term Data. Shore and Beach, Vol. 61, No.2,pp.13-20.

Eckhardt, D.W., Verdin, J.P. and Lyford G.R., 1990. Automated update of an irrigated lands GIS using SOPT HRV imagery. Photogrammetric Engineering and Remote Sensing, 56(11) 1515-1522.

Fenster, M., Dolan, R. and Elder, J., 1993. A new method for predicting shoreline positions from historical data. Journal of Coastal Research, 9, 147-171.

Ferreira, O. and Dias A. J. M., 1992. Dune erosion and shoreline retreat between Aveiro and Cape Mondego (Portugal). Prediction of future evolution. Proceedings. Int. Coastal Congress, Kiel, 187–200.

Ferreira, O., Garcia, T., Matias, A., Taborda, R. and Dias, J.A., 2006. An integrated method for the determination of set-back lines for coastal erosion hazards on sandy shores. Continental Shelf Research, 26, 1030–1044.

Fletcher, C., Rooney, J., Barbee, M., Lim, S.C. and Richmond, B., 2003. Mapping shoreline change using digital orthophotogrammetry on Maui, Hawaii, Journal of Coastal Research Special Issue N° 38, 106–124.

Gonçalves, R.M., Awange, J.L., Krueger, C.P., Heck, B. and Coelho, L.d.S., 2012. A comparison between three short-term shoreline prediction models. Ocean & Coastal Management, 69, 102-110.

Hadjimitsis, D.G., Clayton, C.R.I. and Hope, V.S., 2004. An assessment of the effectiveness of atmospheric correction algorithms through the remote sensing of some reservoirs. International Journal of Remote Sensing, 25(18), 3651-3674.

Hadjimitsis, D.G., Papadavid, G., Agapiou, A., Themistocleous, K., Hadjimitsis, M.G., Retalis, A., Michaelides, S., Chrysoulakis, N., Toulios, L. and Clayton, C.R.I., 2010. Atmospheric correction for satellite remotely sensed data intended for agricultural applications: impact on vegetation indices. Nat. Hazards Earth Syst. Sci., 10, 89-95, doi:10.5194/nhess-10-89-2010.

Hapke, C.J., Reid, D., Richmond, B.M., Ruggiero, P. and List J., 2006. National Assessment of Shoreline Change part 3— Historical shoreline change and associated coastal land loss along sandy shorelines of the California coast. U.S. Geological Survey Open-File Report 2006-1219. [http://pubs.usgs.gov/of/2006/1219].

Li, R., Liu, J. and Felus, Y., 2001. Spatial modelling and analysis for shoreline change and coastal erosion monitoring. Marine Geodesy, 24, 1-12. doi: http://dx.doi.org/10.1080/01490410121502.

Lillesand, T.M. and Kiefer R.W., 1987. Remote Sensing and Image Interpretation, 2nd edition. New York: John Wiley and Sons, 721 p.

Lunetta, R.S. and Elvidge, C.D. (ed.), 1998. Remote Sensing Change Detection: Environmental Monitoring Methods and Application. Chelsea, Michigan, USA: Ann Arbor Press, 318 p.

Mahiny, A.S. and Turner, B.J., 2007. A comparison of four common atmospheric correction methods. Photogrammetric Engineering & Remote Sensing, 73(4), 361–368.

MAMAOT/APA I.P.;, 2012. POOC OVAR-MARINHA GRANDE: VOLUME I. RELATÓRIO: Caracterização e Diagnóstico Prospectivo. CEDRU/ Universidade de Aveiro. Lisboa, Portugal. 829 p.

Martínez, M.L., Intralawan, A., Vázquez, G., Pérez-Maqueo, O., Sutton, P. and Landgrave, R., 2007. The coasts of our world: ecological, economic and social importance. Ecological Economics, 63, 254-272.

Milli, M. and Surace, L., 2011. Le linee della costa. Definizioni, riferimenti altimetrici e modalità di acquisizione dei dati. Città di Castello, Perugia, Italia: Alinea Editrice, 79 p.

Morton, R.A., Miller, T.L. and Moore, L.J., 2004. National assessment of shoreline change: Part 1: Historical shoreline changes and associated coastal land loss along the U.S. Gulf of Mexico. U.S. Geological Survey Open-file Report 2004-1043, 45p.

Mukhopadhyay, A., Mukherjee, S., Mukherjee, S., Ghosh, S., Hazra S. and Mitra, D., 2012. Automatic shoreline detection and future prediction: A case study on Puri Coast, Bay of Bengal, India. European Journal of Remote Sensing, 45, 201-213 doi: 10.5721/EuJRS20124519.

NASAa, 2012, http://landsat.gsfc.nasa.gov/data/reduced.html.

NASAb, 2012, http://landsat.usgs.gov/verify_image_files.php.

Roebeling, P.C., Coelho, C.D. and Reis, E.M., 2011. Coastal erosion and coastal defense interventions: a cost-benefits analysis. Journal of Coastal Research, SI(64), 1415-1419.

Schott, J.R., Salvaggio, C. and Volchok, W.J., 1988. Radiometric scene normalization using pseudoinvariant features. Remote Sensing of Environment, 26, 1–16.

Schowengerdt, R.A., 2007. Remote sensing: models and methods for image processing, Third Edition. San Diego, California, USA: Academic Press, 515 p.

Silva, R., Baptista, P., Veloso-Gomes, F., Coelho, C. and Taveira-Pinto, F., 2009. Sediment grain size variation on a coastal stretch facing the North Atlantic (NW Portugal). Journal of Coastal Research, SI(56), 762–766.

Song, C., Woodcock, C.E., Seto, K.C., Pax Lenney, M. and Macomber, S.A., 2001. Classification and change detection using Landsat TM data: when and how to correct atmospheric effects?. Remote Sensing of Environment, 75, 230–244.

Thieler, E.R., Himmelstoss, E.A., Zichichi, J.L. and Ergul, A., 2009. Digital Shoreline Analysis System (DSAS) version 4.0 — An ArcGIS extension for calculating shoreline change: U.S. Geological Survey Open-File Report 2008-1278. *current version 4.2.

Thomas, T., Phillips, M.R., Williams, A.T. and Jenkins, R.E., 2011. A multi-century record of linked nearshore and coastal change. Earth Surface Processes and Landforms, 36, 995-1006.

Veloso-Gomes, F., Taveira-Pinto, F., Das Neves, L. and Pais-Barbosa, J., 2006. EUrosion - A European Initiative for Suistainable Coastal Erosion. Pilot Site of River Douro - Cape Mondengo and Case Studies of Estela, Aveiro, Caparica, Vale de Lombo and Azores. Porto, Portugal, IHRH, 317 p.

Virdis, S.G.P., Oggiano, G. and Disperati, L., 2012. A Geomatics Approach to Multitemporal Shoreline Analysis in Western Mediterranean: The Case of Platamona-Maritza Beach (Northwest Sardinia, Italy)". Journal of Coastal Research, 28(3), 624 – 640.

White, K. and El Asmar, H.M., 1999. Monitoring changing position of coastlines using thematic mapper imagery, an example from the Nile Delta. Geomorfology, 29, 93-105.

Yang, X. and Lo, C.P., 2000. Relative radiometric normalization performance for change detection from multi-date satellite images. Photogrammetric Engineering and Remote Sensing, 66(8), 967-980.

Yuan, D. and Elvidge C.D., 1996. Comparison of relative radiometric normalization techniques. ISPRS Journal of Photogrammetry and Remote Sensing, 51, 117-126.